URSI GASS 2020, Rome, Italy, 29 August - 5 September 2020

Wideband Interference Mitigation for Synthetic Aperture Radar Data Based on Variational Bayesian Inference

Yi Ding, Weiwei Fan, and Feng Zhou*
Key Laboratory of electronic information countermeasure and simulation technology of ministry of education, Xidian University, 710071 Xi'an, China

Abstract

The existence of wideband interference (WBI) would seriously reduce the SAR imaging quality and the following image interpretation accuracy. However, it is difficult to mitigate WBI owing to its large bandwidth and severe overlapping with useful signal. This paper proposes a WBI mitigation algorithm based on variational Bayesian inference. Firstly, a low-rank matrix factorization model for WBI is established according to the low rank characteristics of WBI in time-frequency domain. Then, we build the Bayesian posterior probability model for the low rank matrix factorization. Finally, the variational Bayesian inference is utilized to estimate the model parameters and reconstruct the WBI. The experimental results of WBI mitigation using measured WBI data acquired by the Sentinel-1 satellite have verified the effectiveness of the proposed algorithm.

1. Introduction

SAR has a wide range of applications in the fields of imaging identification, resource exploration, marine observation, geological mapping, and environmental perception due to its characteristics of all-day, all-weather, high resolution, and long-range. However, the measured SAR data always corrupted by WBI in the same frequency band [1]. The presence of WBI reduce the signal-to-noise ratio of the SAR echo and affects the quality of SAR imaging seriously. Meanwhile, WBI would yield inaccurate estimates of critical Doppler parameters (e.g., centroid and modulation rate), which would result in blurry and defocused SAR images. Moreover, WBI would reduce the accuracy of feature extraction and posing a hindrance to the SAR image interpretation [2]. In order to improve the performance of SAR imaging and image interpretation, it is necessary to develop interference mitigation method for SAR.

Generally, WBI mitigation algorithms can be divided into two categories: data-driven algorithms [2-4] and model-driven algorithms [5-6]. Data-driven interference mitigation algorithms mainly design a reasonable filter and separate the interference and useful signal in a specific domain. Tao *et al.* converted the problem of WBI mitigation into that of narrow-band interference (NBI) mitigation in instantaneous spectrum domain, and the eigensubspace filtering was utilized to mitigate NBI [2]. Zhang *et al*. combined the short-time Fourier transform (STFT) and wavelet transform to map the SAR echo in time domain into the wavelet domain, and WBI mitigation was realized by filtering the corresponding wavelet coefficients of the interference components [3]. However, they have a heavy calculation burden and may cause the signal loss. Fan *et al.* proposed an interference mitigation algorithm based on deep residual network. It performed by abundant time-frequency domain samples of simulated interference to extract interference features [4]. Nevertheless, it heavily relies on the large amount of interference corrupted SAR data. Model-driven interference mitigation algorithms mainly utilize mathematical models to characterize the SAR echoes and optimize the model parameters under specific criteria. Su *et al.* proposed an interference mitigation by utilizing Go Decomposition (GoDec) algorithm, which assumes the interference and useful target signal in time-frequency domain meet low rank and sparseness, respectively [5]. However, the performance of WBI mitigation is not good due to the lack of accuracy of the model. Huang *et al.* proposed a low-rank sparse decomposition based interference mitigation algorithm for SAR, which assumes that the interference is continuity along azimuth direction [6]. However, the continuity of WBI along azimuth direction does not always satisfy. Therefore, we need a more appropriate algorithm for WBI mitigation.

This paper proposes a variational Bayesian inference based WBI mitigation algorithm for SAR. Based on the low-rank characteristics of WBI in the time-frequency domain, a low-rank matrix factorization model is established. Meanwhile, we built a Bayesian posterior probability model for the low-rank matrix factorization problem based on the assumption that the prior of noise follows the Laplace distribution. Moreover, variational Bayesian inference is utilized to estimate model parameters for reconstructing interference.

2. Theory and Methodology

2.1 Signal Modeling

SAR data can be processed and analyzed pulse-by-pulse and the echo can be expressed as a linear superposition of original target echo, interference and additive noise.

$$s(k) = x(k) + i(k) + n(k) \tag{1}$$

where k represents the distance snapshot, and s, x, i, n denote received SAR echo, original target echo, interference and noise, respectively. Compared with the strong WBI, the original target echo has a noise-like distribution, so the echo model can be simplified as:

$$s(k) = i(k) + n_x(k) \tag{2}$$

Where $n_x(k) = n(k) + x(k)$ represents the superposition of useful target echo and noise.

In order to explore the characteristics of the echo, STFT is used to represent the echo into the range time-frequency domain.

$$\mathbf{S} = \mathbf{I} + \mathbf{N} \tag{3}$$

where $\mathbf{S}$, $\mathbf{I}$ and $\mathbf{N}$ denote the time-frequency matrix of the received echo, WBI and noise, respectively. Fig. 1 shows two azimuth echoes from the measured WBI data acquired by Sentinel-1 satellite in time-frequency domain. Obviously, WBI only occupies a limited part in the time-frequency domain, which can be considered as a low-rank matrix.

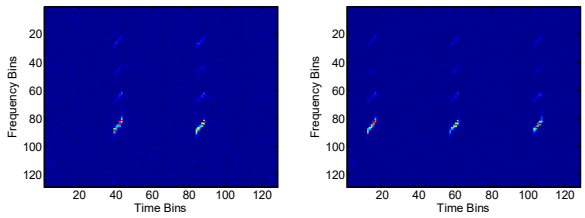

Fig. 1 The representation of two measured WBI-contaminated echoes in the time–frequency domain.

The WBI mitigation problem can be transformed into low-rank matrix recovery problem according to low-rank characteristics of WBI in the time-frequency domain [7], which can be modeled as

$$\min_{\mathbf{U},\mathbf{V}} \left\| \mathbf{S} - \mathbf{U}^H \mathbf{V} \right\|_p \tag{4}$$

Where $\|\cdot\|_p$ is the P-norm of the matrix; $\mathbf{U} \in \mathbb{C}^{r \times Q}$ and $\mathbf{V} \in \mathbb{C}^{r \times T}$ are the factorization of the low-rank matrix, and $r \le \min\{Q,\ T\}$.

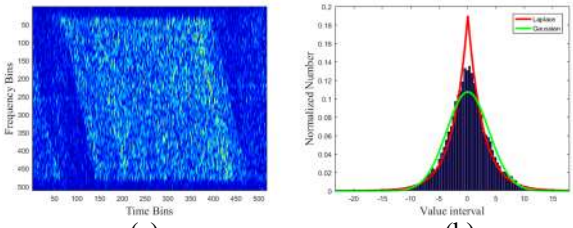

(a) (b)

Fig.2 The probability density of the measured SAR echo in the time-frequency domain. (a) The measured SAR echo in the time-frequency domain. (b) The probability density of the measured SAR echo.

The probability density of the measured SAR echo in the time-frequency domain is shown in Fig.2. Obviously, the probability density of this data is more consistent with the Laplace distribution. Therefore, we can model the noise $\mathbf{N}$ as a Laplace distribution in the time-frequency domain and set the coefficient p in equation (4) to 1. Moreover, we transform the Laplace distribution into a Gaussian scale mixed form [8].

$$p\left(\mathbf{N}_{ij} \middle| 0, \sqrt{\frac{\lambda}{2}}\right) = \int_0^\infty CN\left(\mathbf{N}_{ij} \middle| 0, z_{ij}\right) p\left(z_{ij} \middle| \lambda\right) dz_{ij} \tag{5}$$

where $CN\left(\mathbf{N}_{ij} \middle| 0, z_{ij}\right)$ represents the complex Gaussian distribution with a variance of z_{ij} and zero mean; $p\left(z_{ij} \middle| \lambda\right)$ denotes the exponential distribution with a parameter of λ. In addition, we assume that $\mathbf{u}_i$ and $\mathbf{v}_j$ obey the complex Gaussian distribution which is

$$\begin{aligned} &\mathbf{u}_i \sim CN\left(\mathbf{0}, \tau_{u_i}^{-1}\mathbf{I}\right) \qquad \mathbf{v}_j \sim CN\left(\mathbf{0}, \tau_{v_i}^{-1}\mathbf{I}\right) \\ &\tau_{u_i} \sim \Gamma\left(a_0, b_0\right) \qquad \tau_{v_j} \sim \Gamma\left(c_0, d_0\right), \end{aligned} \tag{6}$$

Where a_0, b_0, c_0, d_0 are the hyperparameters of the Gamma distributions. As following, the Bayesian posterior model is given based on the prior assumptions of the model parameters:

$$\begin{aligned} &p\left(\mathbf{U},\mathbf{V},\boldsymbol{\tau}_\mathbf{u},\boldsymbol{\tau}_\mathbf{v},\mathbf{Z} \middle| \mathbf{S}\right) \propto p\left(\mathbf{U},\mathbf{V},\boldsymbol{\tau}_\mathbf{u},\boldsymbol{\tau}_\mathbf{v},\mathbf{Z},\mathbf{S}\right) \\ &= \prod_{(i,j)\in\Omega} p\left(s_{ij} \middle| \mathbf{u}_i^H \mathbf{v}_j, z_{ij}\right) \prod_{i=1}^{Q} p\left(\mathbf{u}_i \middle| \tau_{u_i}\right) \\ &\times \prod_{j=1}^{T} p\left(\mathbf{v}_j \middle| \tau_{v_j}\right) \prod_{i=1}^{Q} p\left(\tau_{u_i}\right) \prod_{j=1}^{T} p\left(\tau_{v_j}\right) \prod_{(i,j)\in\Omega} p\left(z_{ij}\right) \end{aligned} \tag{7}$$

2.2 **WBI Mitigation Methodology**

As is widely known, the variational Bayesian can be utilized to approximate the full posterior distribution. For the Bayesian posterior of (7), we give the approximate distribution and factorization results:

$$\begin{aligned} q\left(\mathbf{U},\mathbf{V},\boldsymbol{\tau}_\mathbf{u},\boldsymbol{\tau}_\mathbf{v},\mathbf{Z}\right) &= \prod_{i=1}^{Q} q\left(\mathbf{u}_i\right) \prod_{j=1}^{T} q\left(\mathbf{v}_j\right) \\ &\times \prod_{i=1}^{Q} q\left(\tau_{u_i}\right) \prod_{j=1}^{T} q\left(\tau_{v_j}\right) \prod_{ij} q\left(z_{ij}\right) \end{aligned} \tag{8}$$

Parameters are estimated through variational Bayesian inference.

$$\begin{aligned} &q\left(\mathbf{u}_i\right) = CN\left(\mathbf{u}_i \middle| \boldsymbol{\mu}_{u_i}, \boldsymbol{\Lambda}_{u_i}^{-1}\right), q\left(\tau_{u_i}\right) = \Gamma\left(\tau_{u_i} \middle| a_i, b_i\right) \\ &q\left(\mathbf{v}_j\right) = CN\left(\mathbf{v}_j \middle| \boldsymbol{\mu}_{v_j}, \boldsymbol{\Lambda}_{v_j}^{-1}\right), q\left(\tau_{v_j}\right) = \Gamma\left(\tau_{v_j} \middle| c_i, d_i\right) \end{aligned} \tag{9}$$

where

$$\boldsymbol{\Lambda}_{u_i} = E\left[\boldsymbol{\tau}_{u_i}\right] I + \sum_{j=1}^{T} E\left[z_{ij}^{-1}\right] E\left[\mathbf{v}_j \mathbf{v}_j^H\right]$$

$$\boldsymbol{\Lambda}_{v_j} = E\left[\boldsymbol{\tau}_{v_j}\right] I + \sum_{i=1}^{Q} E\left[z_{ij}^{-1}\right] E\left[\mathbf{u}_i \mathbf{u}_i^H\right]$$

$$\boldsymbol{\mu}_{u_i} = \boldsymbol{\Lambda}_{u_i}^{-1} \sum_{j=1}^{T} \mathbf{S}_{ij}^H E\left[z_{ij}^{-1}\right] E\left[\mathbf{v}_j\right], a_i = a_0 + r, b_i = b_0 + E\left[\mathbf{u}_i^H \mathbf{u}_i\right]$$

$$\boldsymbol{\mu}_{v_j} = \boldsymbol{\Lambda}_{v_j}^{-1} \sum_{j=1}^{Q} \mathbf{S}_{ij} E\left[z_{ij}^{-1}\right] E\left[\mathbf{u}_i\right], c_i = c_0 + r, d_i = d_0 + E\left[\mathbf{v}_j^H \mathbf{v}_j\right]$$

$$E\left[z_{ij}\right] = \frac{1}{2}\lambda + \sqrt{\lambda E\left[\left(\mathbf{S}_{ij} - \mathbf{u}_i^H \mathbf{v}_j\right)^2\right]}, \lambda = \frac{\sum_{j=1}^{T}\sum_{i=1}^{Q} E\left[z_{ij}\right]}{QT}$$

Then we reconstruct the WBI and remove the WBI in the

received echo to obtain the useful target echo, it can be expressed as

$$\hat{x}(k) = s(k) - ISTFT\left[\left(\mathbf{U}^{*}\right)^{H}\mathbf{V}^{*}\right] \tag{10}$$

where $\mathbf{U}^{*}$ and $\mathbf{V}^{*}$ represent the final estimation results of low rank factorization. We can obtain well-focused SAR image by performing the WBI mitigation algorithm pulse-by-pulse.

3. Experimental Results

In this section, the effectiveness and robustness of the proposed WBI mitigation algorithm are verified based on the measured WBI-corrupted SAR data. Meanwhile, we compare the WBI mitigation performance with the GoDec algorithm, that the experimental results further demonstrate the superiority of the proposed WBI mitigation method. Moreover, qualitative and quantitative metrics are utilized to evaluate the performance of different interference mitigation algorithms.

The measured SAR data was recorded by C-band Sentinel-1 satellites of the European Space Agency (ESA) with a resolution of $5\text{ m} \times 20\text{ m}$ (range $\times$ azimuth). Fig.3 shows the SAR imaging results by applying different WBI mitigation algorithm. The measured SAR data is acquired by the Sentinel-1A in VH polarization mode. Fig.3 (a) represents the SAR imaging result without applying interference mitigation algorithm. It is obvious that the WBI has completely covered the scene and the SAR image is blurred. Fig.3 (b) and (c) are the SAR imaging results after applying GoDec and the proposed method. The SAR images show that some interference still exist in the scene which resulting in SAR image looks messy after applying the GoDec. For example, the coast contour is not clear enough. However, the SAR image after applying the proposed method looks more clear and the contrast between land and ocean is better.

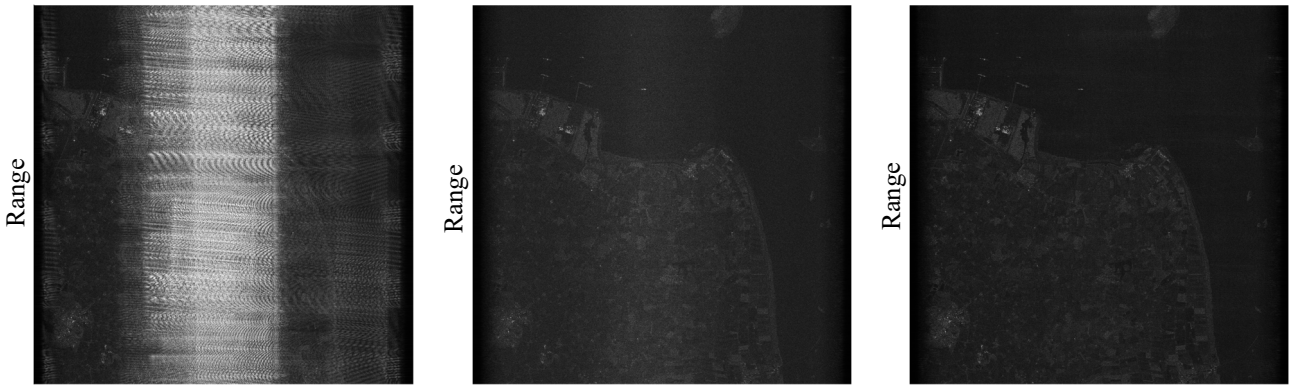

Fig.3 Mitigation results. (a)The SAR image without interference mitigation. (b) The SAR image after applying the GoDec algorithm. (c) The SAR image after applying the proposed algorithm.

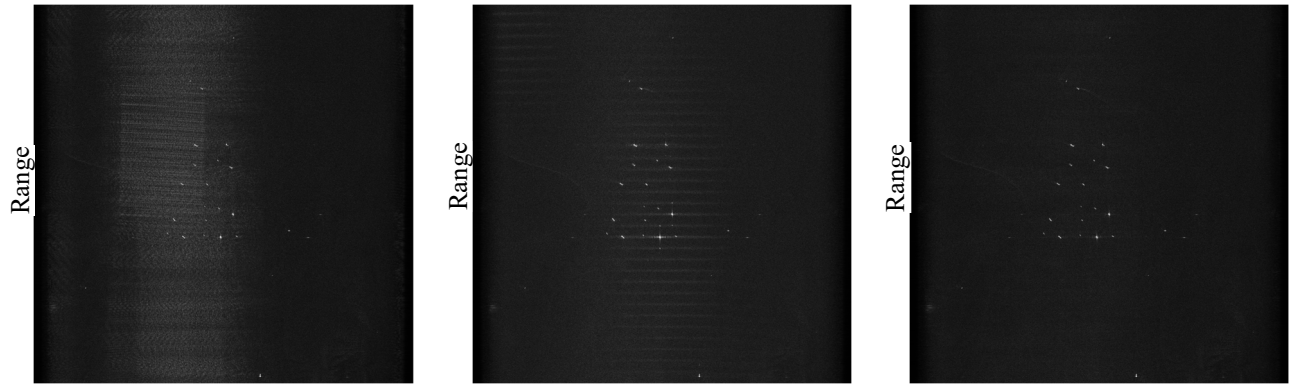

Fig.4 Mitigation results. (a)The SAR image without interference mitigation. (b) The SAR image after applying the GoDec algorithm. (c) The SAR image after applying the proposed algorithm.

To further illustrate the superiority of the proposed method, we performed WBI mitigation experiments for another WBI measure data and the mitigation results shown in Fig.4. This measured SAR data is acquired by the Sentinel-1B in VH polarization mode. Fig.4 (a) represents the SAR imaging result without interference mitigation, in which ships are covered by WBI. Fig.4 (b) and (c) shows the SAR imaging results after applying GoDec and the proposed method. It shows that there is some residual interference in scene and ships are blurred by WBI after applying the

GoDec in Fig.4 (b). However, it can be seen that WBI is well mitigated and ships are well-focused after applying the proposed method.

In order to quantitatively analyze and compare the performance of different interference mitigation algorithm, we utilize a representative multiplicative noise ratio (MNR) as the evaluation index. MNR represents the average energy ratio of the weak scattering area to the strong scattering area in the SAR image. It can be defined as

$$MNR = 10\log_{10}\left(\left(\frac{1}{N}\sum_{n=1}^{N}|I_n|^2\right)\Big/\left(\frac{1}{M}\sum_{m=1}^{M}|I_m|^2\right)\right) \quad (11)$$

where N and I_n represent the number of pixels of the weak scattering area and the corresponding pixel value; M and I_m represent the number of pixels of the strong scattering area and the corresponding pixel value. A smaller MNR demonstrate the contrast of SAR image is stronger, and more SAR image information recovered. Table 1 shows the SAR image quality evaluation. It can be seen that GoDec and proposed algorithm can both improve the quality of SAR image. Meanwhile, the MNR index of the proposed algorithm is better than that of the GoDec algorithm, which is consistent with the qualitative analysis results and indicates that its SAR image has better contrast and clearer contours.

Table 1 SAR image quality evaluation for the measured WBI-contaminated data.

Method / Data	Original	GoDec	Proposed Method
Sentinel-1A VH	5.49dB	-5.87dB	-10.09dB
Sentinel-1B VV	-7.08dB	-12.41dB	-14.90dB

4. Conclusion

This paper proposes a WBI mitigation algorithm based on variational Bayesian inference for SAR. We establish a low-rank matrix factorization model due to the low-rank characteristics of WBI in time-frequency domain. Meanwhile, we adopt the Laplace distribution as prior for noise and derive the posterior probability distribution of the low-rank matrix factorization model. Moreover, Variational Bayesian inference is utilized to estimate the parameters and reconstruct the WBI. Finally, the effectiveness and superiority of the proposed algorithm was verified based on two measured data acquired by the Sentinel-1 satellites. Meanwhile, the MNR is adopted to evaluate the performance of the WBI mitigation. The MNR evaluation results further demonstrate effectiveness of the proposed WBI mitigation algorithm.

5. Acknowledgements

Thanks to all the anonymous reviewers and editors for their comments and suggestions to this article, so that the content of this article can be more rigorous and plentiful. Meanwhile, the authors are grateful for the open-source sentinel-1 satellite SAR data of ESA, which has effectively supported the verification experiments of the algorithm in this paper. This work was supported in part by the National Natural Science Foundation of China under Grant No. 61471284, 61522114, 61631019 and by the NSAF under Grant U1430123; it was also supported by the Foundation for the Author of National Excellent Doctoral Dissertation of PR China under Grant 201448, and by the Young Scientist Award of Shaanxi Province under Grant 2015KJXX-19 and 2016KJXX-82. it was also supported by the Fundamental Research Funds for the Central Universities under Grant No. KJXX1601 and 7214534206.

6. References

1. M. Tao, J. Su, Y. Huang, L. Wang, “Mitigation of Radio Frequency Interference in Synthetic Aperture Radar Data: Current Status and Future Trends,” *MDPI Remote Sens*. **11**, 20, Oct. 2019, pp.2438. doi:10.3390/rs11202438.

2. M. Tao, F. Zhou, Z. Zhang, “Wideband Interference Mitigation in High-Resolution Airborne Synthetic Aperture Radar Data,” *IEEE Trans. Geosci. Remote Sens*. **54**,1, Jan 2016, pp. 74–87. doi:10.1109/TGRS. 2015.2450754.

3. S. Zhang, M. Xing, R. Guo, L. Zhang, Z. Bao, “Interference Suppression Algorithm for SAR Based on Time–Frequency Transform,” *IEEE Trans. Geosci. Remote Sens.* **49**, 10, Oct. 2011, pp.3765–3779. doi:10.1109/ TGRS.2011.2164409.

4. W. Fan, F. Zhou, M. Tao, X. Bai, P. Rong, S. Yang, T. Tian. “Interference Mitigation for Synthetic Aperture Radar Based on Deep Residual Network,” *MDPI Remote Sens*. **11**, 14, Jul. 2019, pp.1654. doi:10.3390 /rs11141654.

5. J. Su, H. Tao, M. Tao, L. Wang, J. Xie, “Narrow-band Interference Suppression via RPCA-Based Signal Separation in Time-Frequency Domain,” *IEEE J. Sel. Topics Appl. Earth Obs. Remote Sens.* **10**, 11, Aug. 2017, pp.5016–5025. doi:10.1109/ JSTARS.2017. 2727520.

6. Y. Huang, L. Zhang, “A Novel Tensor Technique for Simultaneous Narrowband and Wideband Interference Suppression on Single-Channel SAR System,” *IEEE Trans. Geosci. Remote Sens.* **57**, 12, Aug.2019, pp. 9575–9588. doi:10.1109/ TGRS.2019. 2927764.

7. Q. Zhao, D. Meng, Z. Xu, W. Zuo, Y. Yan. “L1-Norm Low-Rank Matrix Factorization by Variational Bayesian Method,” *IEEE Trans. Neural Netw. Learn Syst.* **26**, 4, Jan.2015, pp. 825–839. doi: 10.1109/TNNLS.2014. 2387376.

8. D. F. Andrews and C. L. Mallows, “Scale mixtures of normal distributions,” *J. Roy. Statist. Soc., Ser. B (Methodological),* **36**, 1, 1974, pp. 99 – 102.